Photosynthesis and State Transitions in Mitochondrial Mutants of *Chlamydomonas reinhardtii* Affected in Respiration[1]

Pierre Cardol, Geoffrey Gloire[2], Michel Havaux, Claire Remacle, René Matagne, and Fabrice Franck*

Genetics of Microorganisms (P.C., G.C., C.R., R.M.) and Biochemistry and Photobiology (F.F.), Institute of Plant Biology B22, University of Liège, B–4000 Liège, Belgium; and Commissariat à l'Energie Atomique (CEA)/Cadarache, Direction des Sciences du Vivant, Département d'Ecophysiologie Végétale et de Microbiologie, Laboratoire d'Ecophysiologie de la Photosynthèse, Unité Mixte de Recherche 163 CEA Centre National de la Recherche Scientifique, Univ-Méditérranée CEA 1000, F–13108 Saint-Paul-lez-Durance, France (M.H.)

Photosynthetic activities were analyzed in *Chlamydomonas reinhardtii* mitochondrial mutants affected in different complexes (I, III, IV, I + III, and I + IV) of the respiratory chain. Oxygen evolution curves showed a positive relationship between the apparent yield of photosynthetic linear electron transport and the number of active proton-pumping sites in mitochondria. Although no significant alterations of the quantitative relationships between major photosynthetic complexes were found in the mutants, 77 K fluorescence spectra showed a preferential excitation of photosystem I (PSI) compared with wild type, which was indicative of a shift toward state 2. This effect was correlated with high levels of phosphorylation of light-harvesting complex II polypeptides, indicating the preferential association of light-harvesting complex II with PSI. The transition to state 1 occurred in untreated wild-type cells exposed to PSI light or in 3-(3,4-dichlorophenyl)-1,1-dimethylurea-treated cells exposed to white light. In mutants of the cytochrome pathway and in double mutants, this transition was only observed in white light in the presence of 3-(3,4-dichlorophenyl)-1,1-dimethylurea. This suggests higher rates of non-photochemical plastoquinone reduction through the chlororespiratory pathway, which was confirmed by measurements of the complementary area above the fluorescence induction curve in dark-adapted cells. Photo-acoustic measurements of energy storage by PSI showed a stimulation of PSI-driven cyclic electron flow in the most affected mutants. The present results demonstrate that in *C. reinhardtii* mutants, permanent defects in the mitochondrial electron transport chain stabilize state 2, which favors cyclic over linear electron transport in the chloroplast.

Metabolic processes of photosynthetic organisms depend on the regeneration of ATP through photosynthesis and respiration. Although these two processes are now well understood at the molecular and physiological levels, less is known about their mutual regulation. In eukaryotic cells, complex interactions between photosynthesis and respiration occur because both processes are linked by common key metabolites such as ADP/ATP, NAD(P)H, triose-P, and hexose-P (for review, see Hoefnagel et al., 1998).

When the dependence of respiration on photosynthesis seems to rely essentially on the availability of substrates, the influence of respiration on photosynthesis is suggested to involve complex organizational changes in the PSs, known as state transitions. The transition from states 1 to 2 corresponds to the reversible transfer of a mobile pool of PSII light-harvesting complexes II (LHCII) from PSII to PSI along the thylakoid membrane (state 2 transition) and is triggered by persistent reduction of the plastoquinone (PQ) pool. This reduction causes the activation of an LHCII-kinase interacting with the quinine oxidizing site of cytochrome (Cyt) *b6/f* (for review, see Allen, 1992; Wollman, 2001). Due to its high affinity for the PSI-h subunit, phospho-LHCII then is bound preferentially to PSI and increases the antenna size of this PS. Return to state 1 can be achieved by reoxidation of the PQ pool and is mediated by a permanently active phosphatase.

In the unicellular alga *Chlamydomonas reinhardtii*, a rapid transition toward state 2 can be observed when oxidative phosphorylations are interrupted by anaerobiosis or by addition of uncouplers or inhibitors of mitochondrial electron transport (Bulté et al., 1990). Recent studies in the same organism have shown further that anaerobiosis causes a transient inhibition of oxygen evolution and stimulation of PSI-mediated cyclic electron transport upon state 2 transition (Finazzi et al., 1999, 2002). From these results, Wollman (2001) has inferred that one function of state transitions in *C. reinhardtii* is to modulate the relative rates

[1] This research was supported by Fonds de la Recherche Fondamentale Collective (grant no. 2.4552.01) and by Fonds de la Recherche Fondamentale Collective (grant no. 1.5.145.03 and research fellowship to P.C.). C.R. and F.F. are research associates of the Fonds National de la Recherche Scientifique.

[2] Present address: Virology and Immunology, Institute of Pathology B23, University of Liège, B–4000 Liège, Belgium.

* Corresponding author; e-mail F.Franck@ulg.ac.be; fax 324–3662926.

Article, publication date, and citation information can be found at http://www.plantphysiol.org/cgi/doi/10.1104/pp.103.028076.

of photosynthetic linear and cyclic electron flows. The state transitions would provide a mean of regulating net ATP and NAD(P)H synthesis by the chloroplast because ATP and NAD(P)H are consumed in the Calvin cycle in conditions that favor linear electron transport, whereas ATP resulting from cyclic photophosphorylation can be used in other metabolic processes.

It also has been shown that addition in darkness of uncouplers or inhibitors of mitochondrial electron transport induces a rapid drop in ATP and a stimulation of glycolysis in *C. reinhardtii*. This increases the NAD(P)H level and causes non-photochemical reduction of the PQ pool (Rebeille and Gans, 1988). PQ reduction in the dark was attributed to the process of chlororespiration. Although chlororespiration was discovered more than 20 years ago (Bennoun, 1982), the chloroplastic complexes involved in electron transfer from NAD(P)H to oxygen are not unambiguously identified today. Recent data (for review, see Peltier and Cournac, 2002) suggest that in *C. reinhardtii*, chlororespiratory PQ reduction is catalyzed by a still-unidentified NAD(P)H-PQ oxidoreductase, but a putative ferredoxin-PQ oxidoreductase and a succinate dehydrogenase homologous to mitochondrial complex II may also be involved. A nuclear-encoded plastoquinol oxidase showing restricted homology to the mitochondrial alternative oxidase was detected in *C. reinhardtii* thylakoids and is the most likely candidate to support electron transfer from PQ to oxygen.

The present explanatory frame of the chloroplast response to mitochondrial respiration relies essentially on the analysis of transient changes in photosynthetic parameters upon reduction of mitochondrial electron transport and ATP synthesis by inhibitors or anaerobiosis. Combined with the current model of chlororespiration and with recent understanding of the effects of state transitions, this approach led to a concept of flexibility of photosynthetic electron transport in which the chloroplast appears as a sensor of the ATP status of the cell (Wollman, 2001).

Analyzing photosynthetic electron transport in mutants affected in respiration at various extents constitutes another approach to evaluate chloroplast responses to respiration. In *C. reinhardtii*, a large number of homoplasmic mitochondrial mutants affected in respiration have been isolated (for review, see Matagne and Remacle, 2002; Table I). They are characterized by their null or slow growth when cultivated under heterotrophic conditions (darkness + acetate as an exogenous carbon source). Four mutants (*dum5*, *17*, *20*, and *25*) with point mutation in one of the five *nd* genes (*nd1*, *2*, *4*, *5*, and *6*) of the mitochondrial genome, grow in the dark much slower than the wild-type strain (dark$^{\pm}$ phenotype) and are only affected in the activity of the mitochondrial respiratory chain complex I. The other mutants are unable to grow in the dark (dark^{-} phenotype) because of mutations in the *cob* gene (encoding the apocytochrome b subunit of complex III; mutants *dum1* and *21*) or in the *cox1* gene (coding for the subunit 1 of complex IV; mutants *dum18* and *19*) or because of a large deletion that encompasses *cob* and *nd4* genes (*dum22*). In all these mutants, electron transfer from ubiquinone to molecular oxygen through the alternative oxidase is still functional. The mutants listed in Table I can be classified in three classes based on the putative number of active proton-pumping sites lost in the mitochondrial membrane: loss of one ATP synthesis site (complex I mutants), of two sites (complex III or IV mutants), or of three sites (complexes I + III or I + IV mutants).

In this work, we have analyzed photosynthetic oxygen evolution, state transitions, and cyclic electron transport in the above set of mutants grown under mixotrophic conditions (light + acetate). The data

Table I. *Mitochondrial mutations in C. reinhardtii (dum* [*dark uniparental minus inheritance*]*)*

Mutations	Strain	Growth in the Dark	Biochemical Defect[a]	Gene Mutations	References
Wild-type	2	+	–	–	–
dum 5	641	±	Complex I	−1T, 74 bp downstream from *nd5* stop codon, low amount of *nd5* transcripts	Cardol et al., 2002
dum 17	233	±	Complex I	−1T at codon 143 of *nd6*	Cardol et al., 2002
dum 20	235	±	Complex I	−1T at codon 243 of *nd1*	Remacle et al., 2001
dum 25	228	±	Complex I	Deletion of two of the five codons 199–203 of *nd1*	Remacle et al., 2001
dum 1	165	–	Complex III	*cob* Totally deleted	Matagne et al., 1989
dum 21	271	–	Complex III	1-bp Substitution at codon 166 of *cob*	Remacle and Matagne, 2002
dum 18	236	–	Complex IV	+1T at codon 145 of *cox1*	Colin et al., 1995
dum 19	238	–	Complex IV	−1T at codon 152 of *cox1*	Colin et al., 1995
dum19/25	300	–	Complexes I and IV	*cf dum19* and *dum25* mutations	Remacle et al., 2001
dum 22	662	–	Complexes I and III	*cob* and 3′ End of *nd4* deleted	Remacle and Matagne, 2002

[a] All the mutants lack the activity of the mentioned complex, except *dum*5, which shows very low complex I activity.

obtained allow us to evaluate current ideas on the impact of respiration on photosynthetic electron transport and provide quantitative relationships between these processes.

RESULTS

Respiration Rates Strongly Correlate with Relative Quantum Yields of Linear, Photosynthetic Electron Transport

Polarographic measurements of oxygen exchange rates in darkness and in light of increasing photosynthetic photon flux densities were performed with wild-type cells and mutant cells affected in various complexes of the mitochondrial electron transport respiratory chain (Table I). Light saturation curves of photosynthetic oxygen evolution were established and compared on a chlorophyll (Chl) basis. When comparing the light curve obtained with the wild type with that of a double mutant (*dum19/25*) deprived of complexes I and IV activities, clear differences appeared both in the maximum rate of oxygen evolution in saturating light (V_{max}) and in the initial slope of the light curve (α') up to 50 μmol m^{-2} s^{-1} (Fig. 1). In the double mutant, V_{max} and α' were reduced by about 40% and 80%, respectively. Because α' is proportional to the quantum yield of linear, photosynthetic electron transport from molecular oxygen to $NADP^+$, it represents an important parameter of photosynthetic efficiency. It was measured in all the mutants and plotted as a function of the rate of dark respiration (Fig. 2). In this plot, the three categories of mutants (complex I mutants; mutants of the Cyt pathway, i.e. complex III or complex IV mutants; and double mutants) distribute into three groups of points along a single relationship between photosynthetic quantum yield and dark respiration rate.

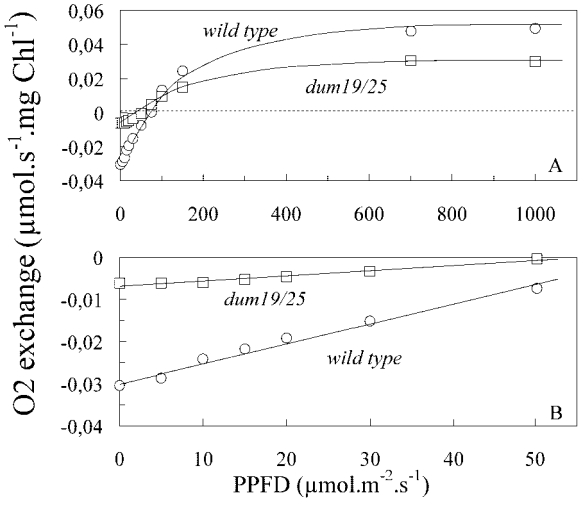

Figure 1. Light saturation curves of oxygen evolution in cells of wild-type and *dum*19/25 double mutant (lacking complexes I and IV). A and B, Two scales of photosynthetic photon flux densities.

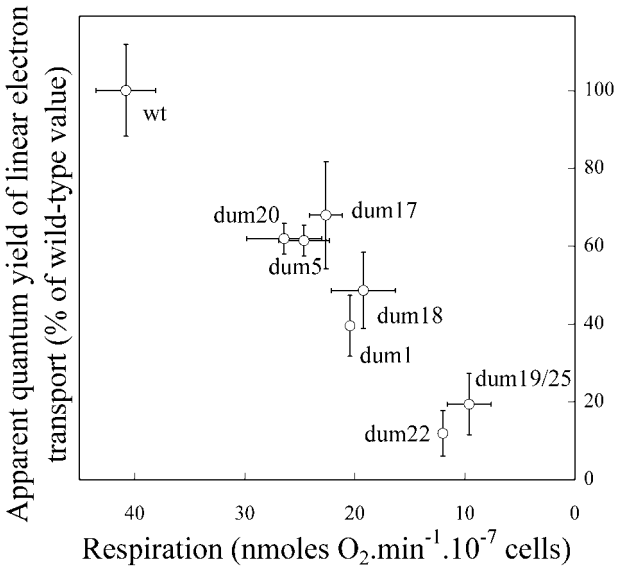

Figure 2. Relationship between the rate of dark respiration and the apparent quantum yield of oxygen evolution (estimated from the initial slope of the light saturation curves and expressed in percentage of the wild-type control).

The respiration rate values reflect the effects of the loss of different mitochondrial electron transporters. Mutants of complex I still show substantial respiration due to the presence of multiple NADH-dehydrogenases (Cardol et al., 2002). Mutants of the Cyt pathway, which rely solely on alternative oxidase to reduce oxygen, are somewhat more affected, whereas double mutants show very weak oxygen uptake rates. Mitochondrial oxidative phosphorylation capacity must decrease in the same order because the number of operating phosphorylating sites decreases from one group to another (three in wild type, two in complex I mutants, one in mutants of the Cyt pathway, and none in double mutants).

Mitochondrial Mutants Show Similar Composition of Their Photosynthetic Apparatus and Have Moderately Reduced ATP Levels Compared with Wild Type

The large effects of mitochondrial mutations on photosynthetic electron transport outlined above can be due to quantitative modifications of photosynthetic pigment-protein complexes and/or to changes in their organization or activities. Therefore, it was important to evaluate the concentrations of photosynthetic constituents on a cell basis. Simple spectrophotometric measurements of total Chl concentration in ethanolic extracts gave a wild-type value of 23 μg Chl per 10^7 cells with no difference higher than 12% in the different groups of mutants. This was further confirmed by HPLC analysis, which showed no significant differences in Chl or carotenoid contents (data not shown). The Chl *a*/*b* ratio was fairly con-

stant with a mean value of 2.5, which indicated no obvious changes in PSI/PSII stoichiometry. In crude membranes from wild-type cells, the concentrations of P700 (PSI), Cyt b559 (PSII), and Cyt f (Cyt b6/f complex) estimated by redox difference spectroscopy were around 2 nmol μmol^{-1} Chl in each case. No significant differences were found for double mutant cells (data not shown). We also found that cellular concentrations of total proteins did not vary by more than 20% in different groups of mutants compared with wild type (around 130 μg protein per 10^{-7} cells). This allowed us to express any activity or concentration indifferently on a cell, Chl or protein basis.

Because the mutants are impaired in at least one mitochondrial phosphorylating site, we expected significant reduction of the cell ATP concentrations compared with wild type. However, ATP measurements by the luciferase assay on extracts of illuminated cells showed relatively modest decreases (Fig. 3). The wild-type cell ATP concentration was 103 $\pm$ 23 nmol mg Chl^{-1}, a value comparable with previously published data (Finazzi et al., 1999). Complex I mutants showed no significant difference compared with wild type. ATP concentration was reduced in mutants of the Cyt pathway and in double mutants, but even in the latter, it was more than 60% compared with wild type.

The Excitation Energy Distribution Is Shifted to "State 2" in White Light, and PSI Light Fails to Promote Transition to "State 1" in Mitochondrial Mutants

State transitions were monitored by measurements of steady-state Chl fluorescence spectra at 77 K. Excitation in the Chl Soret band produces PSII and PSI fluorescence bands at 685 and 715 nm, respectively. In wild-type cells frozen to 77 K under the white light used for growth (70 μmol m^{-2} s^{-1}), the two bands had similar amplitudes (Fig. 4A). Incubation under flushing nitrogen during 20 min in darkness before freezing caused an increase of the relative amplitude of the PSI band, reflecting transition to state 2 caused by PQ reduction. Full transition to state 1, detected as a decrease of the relative amplitude of the PSI band, was obtained by pre-illuminating the cells with PSI light ($\lambda > 705$ nm) of 60 W m^{-2} for 5 min, which causes oxidation of the PQ pool. The same effect was observed when the cells were pre-illuminated by white light of 70 μmol m^{-2} s^{-1} in the presence of DCMU, a treatment that also results in PQ oxidation due to PSII inhibition by DCMU (Fig. 4A).

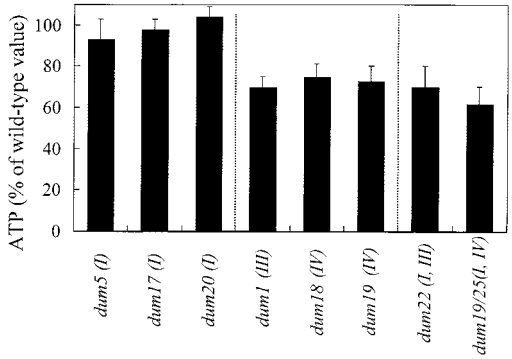

Figure 3. Cellular ATP concentrations of mitochondrial mutants, expressed in percentage of the wild-type control. Cells were fixed under illumination with white light of 70 μmol m^{-2} s^{-1}, as used during growth.

In double mutant cells (*dum* 19/25), a high relative amplitude of the PSI band, indicative of state 2, was found already in cells frozen in white light (Fig. 4A). It was only slightly increased after dark incubation under nitrogen. Pre-illumination by PSI light of $\lambda >$ 705 nm, instead of promoting transition to state 1 as in wild-type cells, caused a slight increase of the 715-nm band. This indicates a slight shift toward state 2, which can probably be explained by residual PSII excitation. Transition to state 1 was only observed after pre-illumination by white light in the presence of DCMU. Thus, compared with wild type, the double mutant appears closer to state 2 in continuous white light and shows transition to state 1 only in conditions that allow strong excitation of PSI.

To compare the whole set of mutants with regard to their ability to perform state transitions, the F715 to F685 ratio was used as an indicator of the state of excitation energy distribution and was measured in untreated cells and in state 1 or 2 conditions as above (Fig. 4B). Compared with wild type, complex I mutants (*dum*5, *dum*17, *dum*20, and *dum*25) showed already significant shifts toward state 2 when frozen under white light (untreated) or in state 1 conditions. In these mutants, the transition to state 1 was barely detected. Similarly, mutants of the Cyt pathway (*dum*1 for complex III and *dum*18 and *dum*19 for complex IV) did not show transition to state 1. In state 2 conditions, these mutants further showed a higher F715 to F685 ratio than the wild type in the same conditions. Double mutants (*dum*19/25 and *dum*22), when frozen in white light, showed a F715 to F685 ratio that was as high as for the wild type in state 2 conditions. This ratio further increased in state 2 conditions and could reach a value well beyond the one found for the wild type (2.25 instead of 1.5 for *dum*22). Thus, one concludes that excitation of PSI by 60 W m^{-2} during 15 min (state 1 conditions) does not promote state 1 in most of the mutants. However, transition to state 1 was promoted by pre-illumination by white light in the presence of DCMU. On the other hand, the most affected mutants can show a significantly higher F715 to F685 ratio in state 2 compared with wild type.

State transitions are caused by phosphorylation (state 2) or dephosphorylation (state 1) of a set of mobile LHCs of the *lhcb* family. In *C. reinhardtii*, state 2 transition involves phosphorylation of LHCII polypeptides and the minor Chl *a*/*b*-binding CP26 and CP29 polypeptides at a Thr residue (Wollman

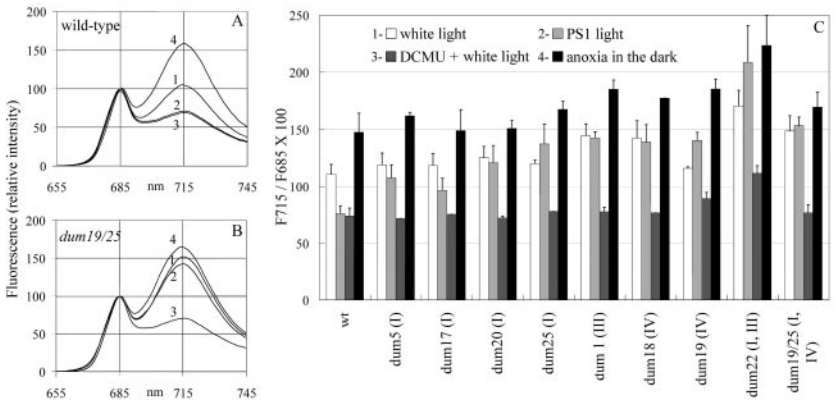

Figure 4. Analysis of state transitions by 77 K fluorescence spectroscopy. A, Fluorescence emission spectra (77 K) of the wild-type control and of the *dum*19/25 double mutant (lacking complexes I and IV). Different pretreatments were applied to cell suspensions before freezing: 1, control under white light of 70 μmol m^{-2} s^{-1}; 2, illumination by PSI light ($\lambda > 705$ nm) of 60 W m^{-2} during 15 min; 3, illumination by white light of 70 μmol m^{-2} s^{-1} in the presence of 10 μM 3-(3,4-dichlorophenyl)-1,1-dimethylurea (DCMU); and 4, dark incubation under nitrogen atmosphere during 20 min. B, F715 to F685 ratios measured in the same conditions for the wild type and for the indicated mutants.

and Delepelaire, 1984), which can be detected on immunoblots using an anti-phospho-Thr antibody (Fleischman et al., 1999). In membranes of wild-type cells (Fig. 5), we detected two main bands of 26- and 34-kD apparent molecular mass. Because the number and position of phospho-Thr-containing polypeptides are highly dependent on the gel system used, we will refer to them collectively as antenna phosphoproteins. These two polypeptides were heavily phosphorylated in state 2 conditions (anoxia in darkness). The phosphorylation level was significantly lower when cells were frozen under the white light (70 μmol m^{-2} s^{-1}) used for growth, and no antenna phosphoprotein could be detected in either of the two conditions that promote transition to state 1 (PSI light pre-illumination or white light pre-illumination in the presence of DCMU).

Complex I mutants such as *dum*17 already showed a clearly different behavior because pre-illumination by PSI light did not cause significant labeling attenuation, in contrast to wild type. The *dum*1 mutant (lacking complex III) and the *dum*19/25 double mutant (lacking complexes I and IV) exhibited strong phosphorylation under white light, PSI light, or anoxia in the dark but still showed a marked decrease of phosphorylation level when pre-illuminated with white light in the presence of DCMU.

The persistence of phosphorylated antenna proteins in PSI light seen in the mutants was consistent with their inability to perform transition to state 1 in these conditions, as concluded from 77 K fluorescence measurements.

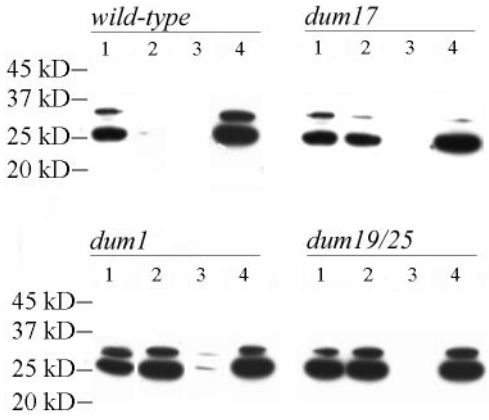

Figure 5. Immunoblot detection of phosphorylated LHCs of the wild-type control and of the *dum*17, *dum*1, and *dum*19/25 mutants lacking complex I, complex III, and complexes I and IV, respectively. Immunoblotting was performed on 10 μg of membrane proteins using an antibody against phospho-Thr. Different pretreatments were applied to cell suspensions before membrane isolation: 1, control under white light of 70 μmol m^{-2} s^{-1}; 2, illumination by PSI light ($\lambda > 705$ nm) of 60 W m^{-2} during 15 min; 3, illumination by white light of 70 μmol m^{-2} s^{-1} in the presence of 10 μM DCMU; and 4, dark incubation under nitrogen atmosphere during 20 min.

The Low Rate of "State 1" Transition in the Mutants Is Correlated with a Higher Reduction Level of the PQ Pool

In *C. reinhardtii*, as in higher plants, state transitions are controlled primarily by the redox status of the PQ pool. Previous studies have indicated that inhibitors of the mitochondrial electron transport or ATP synthesis cause a rapid non-photochemical reduction of the PQ pool that results in transition toward state 2 (Bulté et al., 1990). To evaluate the redox status of the PQ pool in the set of mitochondrial mutants studied here, we have performed fluorescence induction measurements at room temperature. During a saturating red light pulse (1,000 μmol m^{-2} s^{-1}) given after a short dark adaptation (5 min), wild-type cells showed a ratio of variable to maximal fluorescence (F_v/F_m) around 0.6 in our experimental conditions (Fig. 6C). Single mutants showed significantly reduced F_v/F_m ratios, which is another indication of a transition to state 2 (Finazzi et al., 1999). In double mutants, this ratio was reduced to 0.3, a value close to the one obtained with wild-type cells placed in state 2 by a 5-min dark incubation in the absence of oxygen (data not shown).

The redox state of the PQ pool can be evaluated semiquantitatively on the basis of fluorescence induction measurements performed in the absence and in the presence of DCMU, an inhibitor of PSII-driven electron transport between the bound plastoquinone

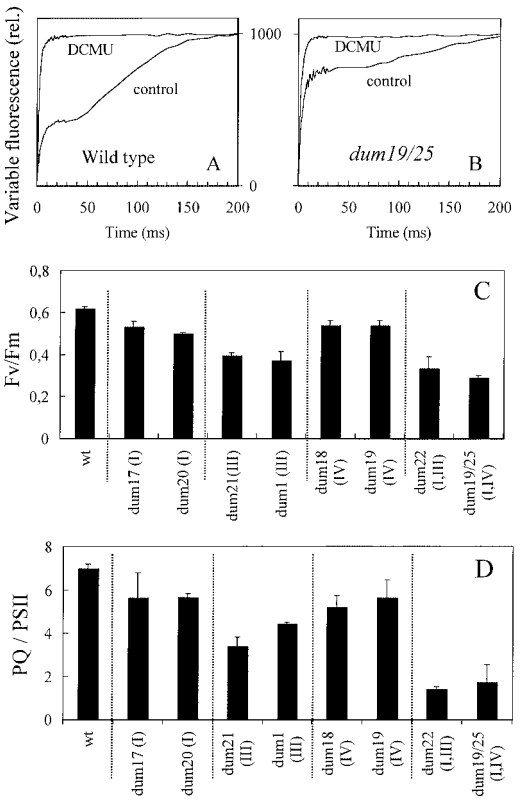

Figure 6. Analysis of the redox state of PQs from fast fluorescence induction curves recorded in the absence or in the presence of DCMU (10 μM) after 5 min of dark adaptation. A and B, Variable fluorescence traces (averages of four recordings) of cell suspensions of the wild-type control and of the *dum*19/25 double mutant lacking complexes I and IV (only the variable part of the signal, from F_o to F_m, is shown here after normalization to F_m). C, F_v/F_m ratios in the absence of DCMU. D. Apparent numbers of oxidized PQ per PSII reaction center, calculated from the complementary areas over the fluorescence induction curves.

in PSII (Q_A) and external PQ acceptors. Early studies have shown that the area between the fluorescence rise curve and its F_m asymptot (complementary area) is proportional to the number of electrons transported through the PSII reaction center during the induction phenomenon (Malkin and Kok, 1966). As a consequence, the number of oxidized PQ molecules per active PSII reaction center can be derived from the ratio of the complementary area measured in the absence and in the presence of DCMU, as shown in Figure 6, A and B, for wild-type and *dum*19/25 cells, respectively. This ratio is best measured when PQ reoxidation by PSI is abolished, for instance by using a *C. reinhardtii* mutants lacking Cyt *b6/f*. In this case, oxidized PQ values around 5 have been found (Bennoun, 2001). By using an excitation light of 1,000 μmol m^{-2} s^{-1}, which allowed us to approach full PQ reduction at F_m (judging from the maximal F_m/F_o ratio) and, thus, minimize the effect of PQ reoxidation, we obtained an average value around 7 in wild-type cells (Fig. 6D). Complex I mutants showed slightly lower average values. A significant reduction was observed in complex III mutants (average values around 4), whereas complex IV mutants behaved like complex I mutants. Double mutants showed the lowest values (around 1.5 in average; Fig. 6D).

Because the measurements were performed after a 5-min dark adaptation, these results indicate that significant non-photochemical reduction of the PQ pool occurs in mutants and that its rate is dependent on the extent of inhibition of respiration caused by the mitochondrial mutations. The differences between the behavior of complex III and complex IV mutants in this respect and in the F_v/F_m ratio, however, are unexpected and may point to specific effects of deficiencies in one or the other complex (see "Discussion").

An increased rate of non-photochemical PQ reduction may explain why PSI light fails to promote state 1 transition in the mutants, as evidenced by 77 K fluorescence spectra measurements and detection of phosphorylated LHCII proteins. For state 1 transition to occur, the rate of PQ oxidation in PSI light must overbalance the rate of non-photochemical PQ reduction in such a way that net PQ oxidation is achieved. When the rate of non-photochemical PQ reduction is high, the rate of PSI excitation by the poorly absorbed light at wavelength beyond 705 nm may be too low, and PQ may remain largely reduced. On the other hand, white light of moderate intensity will be better absorbed by PSI and cause higher rates of PQ oxidation in the presence of DCMU, leading to state 1. The persistence of state 2 in PSI light would simply reflect a lower yield of state 1 transition in the mutants. We verified this point by comparing the rate of state 1 transition under white light of low intensity (10 μmol m^{-2} s^{-1}) in wild-type or mutant cells in the presence of DCMU. For this purpose, the kinetics of state 1 transition were monitored by continuous fluorescence measurements at room temperature using modulated excitation. State 1 transition causes an increase of the maximal fluorescence yield (F_m), which can be followed by applying saturating pulses during continuous measurements of fluorescence yield (Delepelaire and Wollman, 1985; Finazzi et al., 1999). The time course of typical experiment is shown in Figure 7A for wild type and the *dum*19/25 mutant. After a 5-min dark adaptation, cells were illuminated by actinic white light of 10 μmol m^{-2} s^{-1} during 5 min; then, light intensity was increased to 100 μmol m^{-2} s^{-1} to complete state 1 transition. The F_m changes during low-light excitation were monitored by exposure to repeated 1-s saturating pulses of 100 μmol m^{-2} s^{-1}. Wild-type cells, but not double mutant cells, showed a steady F_m increase during excitation by white light of 10 μmol m^{-2} s^{-1}. Both cell types reached maximal F_m under 100 μmol m^{-2} s^{-1}. In wild-type cells, the initial state of energy distribution was intermediate between states 1 and 2, whereas double mutant cells were close to state 2 (77

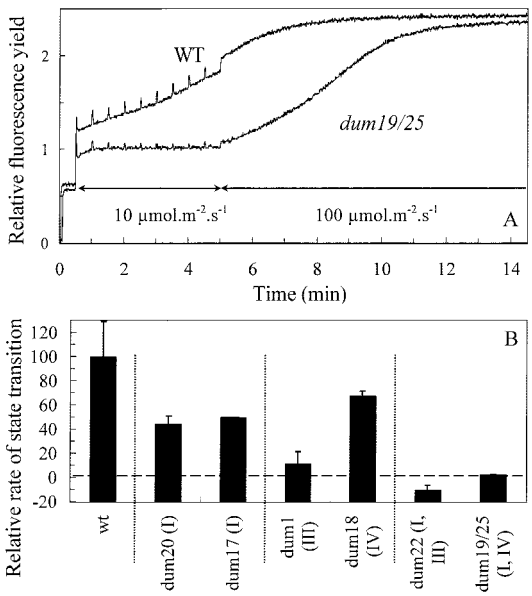

Figure 7. Slow changes in room temperature fluorescence quantum yield associated with state 1 transition during illumination by white light in the presence of 10 μM DCMU. A, Recordings of the modulated fluorescence signal in wild-type and *dum*19/25 cells. Cells are illuminated by 10 μmol m^{-2} s^{-1}, and 1-s saturating pulses of 100 μmol m^{-2} s^{-1} are given every 1 min to record F_m. After approximately 5 min, the photosynthetic photon flux density (PPFD) is kept continuously at 100 μmol m^{-2} s^{-1}. B, Initial rate of F_m increase under 10 μmol m^{-2} s^{-1} in wild-type and mutant cells, expressed in percentage of the wild-type control.

K fluorescence; data not shown). Thus, the measured kinetics followed a larger part of the state 1 transition process in the mutant. The stability of F_m under low actinic light and its increase under stronger light indicate the high light requirement for initiating state 1 transition in the mutant. We quantified the relative rate of state 1 transition in different mutants by the ratio of the initial rate of F_m increase under low actinic light (10 μmol m^{-2} s^{-1}) over the maximal F_m value reached at state 1. The variations of this ratio from one mutant to another, shown in Figure 7B, are in good agreement with variations of the PQ redox state evaluated by measurements of complementary areas over the fluorescence induction curve (Fig. 6D). This confirms the close link between state transitions and non-photochemical PQ reduction.

Photo-Acoustic Measurements of Energy Storage (ES) under PSI Light Indicate an Increased Rate of Cyclic Electron Flow in the Most Affected Mutants

The physiological role of state transitions has been reevaluated recently and suggested to provide a regulation mechanism to control the relative rates of linear and cyclic electron transport pathways in chloroplasts in response to the ATP status of the cell (Wollman, 2001). As we show here, respiratory mutants of *C. reinhardtii* are shifted to state 2 and show decreased quantum yields of linear electron transport compared with wild type. To determine whether these modifications are accompanied by increased rates of cyclic electron transport, we performed photo-acoustic measurements of thermal dissipation by PSI. It was shown previously that ES under weak modulated PSI light, measured as the relative amplitude of the photothermal signal rise caused by saturating light, reflects the yield of PSI-driven cyclic electron transport (Malkin and Canaani, 1994). We measured ES as a function of the modulation frequency in wild-type and in double mutant (*dum*19/25) cells deposited on a nitrocellulose filter and treated as solid samples. In both cases, a biphasic relationship between ES and modulation frequency was observed (Fig. 8A), as already described for *C. reinhardtii* cells (Canaani et al., 1989). ES was significantly higher at all frequencies in double mutant cells, but the increase was more pronounced at high frequencies (beyond 150 Hz). When comparing ES measured at 200 Hz in different mutants (Fig. 8B), a significant increase was found for complex III, complex IV, and double mutants but not for complex I mutants, which were close to wild type. The highest stimulation of ES, around 40% compared with wild type, was found for *dum*1 (complex III) and *dum*19/25 (complexes I and IV) mutants. It is noteworthy that complex IV mutants (*dum*19 and *dum*18) were, again, less stimulated than the complex III mutant (*dum*1).

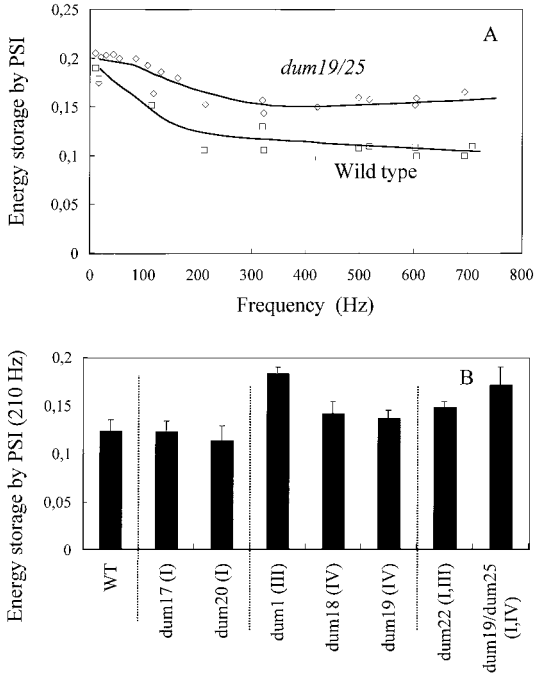

Figure 8. PSI ES measured from the photo-acoustic photothermal signal measured under modulated PSI light ($\lambda > 715$ nm). A, ES as a function of the modulation frequency of excitation light in cells of the wild-type control and of the *dum*19/25 mutant lacking complexes I and IV. B, ES values of cells of the wild type and of the indicated mutants.

DISCUSSION

Previous works have shown that the respiratory mutants used in this study are unable to grow in darkness or grow poorly when supplied with acetate (Matagne and Remacle, 2002; see Table I). This light requirement indicates that photosynthetic phosphorylations are necessary to compensate the reduction in rate of oxidative phosphorylation in the mutants. In the chloroplast, ADP phosphorylation can be energetically coupled to either linear or cyclic (PSI-mediated) electron flow. However, it is generally admitted that most of the ATP produced through linear electron flow is consumed by the reductive pentose pathway, the operation of which necessitates a ratio of three ATPs to two NADPHs for every fixed CO_2. In linear electron transport from water to $NADP^+$, the ATP/NADPH ratio is somewhat lower (1.28; Joliot and Joliot, 2002). Therefore, it is likely that ATP synthesis driven by cyclic electron flow is required to support growth of the mutants, especially those in which oxidative phosphorylations are completely impaired.

The very strong dependence of oxygen evolution on respiration found here shows that in the double mutants, which have lost the ability for oxidative phosphorylations, the quantum efficiency of linear electron transport is reduced to 15% to 20% of that of the wild type. This suggests that in this case, light energy is used mainly in cyclic electron transport. The response of the other mutants is roughly proportional to the expected decrease in oxidative phosphorylation due to the loss of complex I or either complex III or IV. State transition experiments and PQ reduction estimations indicate that the inhibition of oxygen evolution in the mutants is due to a shift to state 2 caused by non-photochemical reduction of the PQ pool. Altogether, the results are in general agreement with the model recently proposed by Wollman (2001) in which state transitions allow modulation of the relative rates of linear and cyclic electron flows in response to the ATP status of the cell. They further show the ability of this regulatory mechanism to ensure survival and growth in conditions of restricted mitochondrial activity. Previous characterization has shown, however, that under mixotrophic conditions (light + acetate), mitochondrial mutants display somewhat limited growth compared with wild type in the light (Remacle et al., 2001), with mutants of complex I being less affected than mutants of the Cyt pathway or double mutants. The extent to which cyclic photophosphorylation compensates for the reduction of mitochondrial ATP synthesis must be one of the factors that determine growth rate. From the present results, it appears that compensation is only partial because the cellular ATP levels of the mutants are lower than that of wild type (except for complex I mutants). On the other hand, the reduction in the quantum yield of photosynthetic linear electron transport will limit photosynthetic carbon fixation in moderate light and contribute to the reduction in growth rate. Obviously, each mutant reaches an optimum steady-state equilibrium by adjusting photosynthetic carbon fixation and cyclic photophosphorylation in response to mitochondrial activity.

In this work, ES under PSI light was measured as indicator of cyclic electron flow. Significant ES was detected in the wild type, which indicates significant cyclic electron transport upon exclusive PSI excitation in state 1. Its biphasic dependence on the modulation frequency of the exciting light values most probably indicates the occurrence of two different cyclic electron pathways with different kinetics, as suggested by a recent study on tobacco (*Nicotiana tabacum*) chloroplasts (Joët at al., 2002). Following the interpretation from this study, ES at high frequency (200 Hz or more) is mainly due to NAD(P)H-dependent cyclic electron flow, whereas at low frequency, an additional contribution from cyclic electron flow involving ferredoxin and a putative ferredoxin-PQ oxidoreductase is involved. The higher stimulation found in the high frequency region compared with the low-frequency region in the mutants suggests that essentially the rate of the NAD(P)H-dependent pathway is increased. In this region, the enhancement is not detected in complex I mutants and it varies from 20% to 50% in the others. Because the measuring light (>715 nm) excites preferentially Chl located in the core of PSI, this enhancement cannot be caused by an increased antenna size in state 2 but rather is due to faster intrinsic rates of electron transport steps. This effect is most probably due to the redistribution of Cyt *b6/f* from appressed to nonappressed thylakoid regions upon state 2 transition, shown before by Vallon et al. (1991). This redistribution will favor electron transport between Cyt *b6/f* and PSI by plastocyanin because PSI is exclusively located in appressed thylakoid regions (Vallon et al., 1986; Wollman, 2001). In this context, a recent kinetic study on higher plant thylakoids strongly suggested that cyclic electron flow necessitates physical connection between PSI and Cyt *b6/f* (Joliot and Joliot, 2002).

To evaluate the effective stimulation of cyclic electron transport, the increased PSI antenna size due to state 2 transition must be taken into account together with the stimulation of ES. Previous studies have shown that in *C. reinhardtii*, a shift to state 2 corresponds to the displacement of 80% of the LHCII from PSII to PSI, leading to an increase of PSI antenna size of 50% in red light compared with state 1 (Delosme et al., 1996). This increase, together with the 50% stimulation of ES in the most affected mutants, would lead to more than doubling the rate of cyclic electron flow under constant excitation conditions.

The large effect of state transitions on energy distribution between PSs explains the strong impact of respiration on linear electron flow measured here as

oxygen evolution. However, significant apparent quantum yields of oxygen evolution (10%–20% of wild type) were measured in double mutants, which are deficient in mitochondrial ATP synthesis and remain in state 2 in the light. Thus, in contrast to earlier findings on wild-type cells subjected to anaerobiosis in similar culture conditions (Finazzi et al., 1999), we find that a basal level of oxygen evolution persists in state 2. This apparent discrepancy has to be found in the different experimental approaches used to reach state 2. In the present work, a basal level of respiration (essentially due to alternative pathways) is maintained in the double mutants, whereas anaerobiosis leads to a complete inhibition and may have additional effects. The persistence of low quantum yields of oxygen evolution in double mutants results in maximal oxygen values close to those of wild type in saturating light. It may allow the avoidance of PSII photo-inhibition during long-term exposure to moderate light. No indication of PSII photo-inhibition was apparent from the values of maximal variable fluorescence, which were similar in double mutants or in wild type in state 2.

In this study, we found that mutants of complex IV were less affected than mutants of complex III when the PQ redox status, the ability to undergo state 1 transition in weak light, and the ES by PSI were investigated. This is unexpected because complex III or IV mutants are in principle equivalent on the basis of mitochondrial respiration defect. The Cyt pathway is inactive in both cases, and we checked that the ATP level in dark-adapted (90 min) cells did not differ significantly (values of 65% to70% of wild type), thus indicating no visible difference in oxidative phosphorylation ability (data not shown). Interestingly, it was found recently that complex IV is specifically involved in ascorbate synthesis in higher plant mitochondria (Bartoli et al., 2000). In plants, the last step of ascorbate biosynthesis consists of the oxidation of L-galactono-lactone by a membrane dehydrogenase that couples L-galactono-lactone oxidation to the reduction of Cyt *c* (Wheeler et al., 1998). Reduced Cyt *c* is then oxidized by complex IV. In potato mitochondria, inhibition of complex IV by cyanide strongly reduces ascorbate synthesis (Bartoli et al., 2000). One can hypothesize that the same pathway occurs in *C. reinhardtii* and that mitochondrial ascorbate synthesis is specifically inhibited in complex IV mutants. Therefore, it is tempting to propose that in wild type and in mutants not affected in complex IV, interactions of ascorbate with the photosynthetic electron transport chain participate in non-photochemical PQ reduction and initiate partial state 2 transition. Complex III mutants might even show higher responses because a stimulation of ascorbate synthesis by antimycin A (an inhibitor of Cyt *c* reduction by complex III) was reported in potato mitochondria (Bartoli et al., 2000). However, to our knowledge, reduction of PQ by ascorbate in thylakoids has not been reported, although chemical reduction of extracted PQ by ascorbate is common routine. Other interactions with photosynthetic electron transport may be involved, such as with the PSI-reducing side and the PSII-oxidizing side (Smirnoff, 2000). Further investigation is required to explore these possibilities in the context of the interactions between mitochondria and chloroplast.

Non-photochemical reduction of the PQ pool appears to play a key role in the transition to state 2 observed in the mutants. This was also observed in a previous work using inhibitors of respiration or of oxidative phosphorylation in wild-type cells or in one of the complex III mutants used here (*dum1*; Bulté et al., 1990). The high rate of "dark" PQ reduction in mitochondrial mutants is documented here by high levels of reduced PQ estimated from complementary fluorescence areas in dark-adapted cells. It explains in part the low quantum efficiency of state 1 transition in the mutants. On the other hand, increased rates of cyclic electron transport due to relocalization of Cyt *b6/f* in nonappressed thylakoid regions will also slower PQ oxidation. Non-photochemical PQ reduction has been ascribed to a chlororespiratory electron flow from NAD(P)H to oxygen (for review, see Peltier and Cournac, 2002). High PQ reduction level in mitochondrial mutants can be sustained by stimulated NADH production through glycolysis due to lower ATP levels (Rebeille and Gans, 1988). However, ATP deficiency is partly compensated by increased cyclic photophosphorylation in steady-state conditions, and clear differences in cellular ATP levels were only found in mutants of the Cyt pathway. Therefore, increased NAD(P)H levels resulting directly from lower rates of mitochondrial NADH oxidation must also be considered as a cause of increased PQ reduction rate in the mutants.

In conclusion, the use of mutants with permanent defects in the mitochondrial electron transport chain allows to demonstrate that photosynthetic electron transport is tightly controlled by respiration in *C. reinhardtii*. This work further emphasizes state transitions as a regulatory process important for modulating cyclic and linear chloroplastic electron transport and maintaining viability when mitochondrial ATP synthesis is impaired. In the future, the double mutants exhibiting high non-photochemical PQ reduction rate should become useful tools for further investigating the still poorly characterized electron transport pathways involved in chlororespiration in this alga.

MATERIALS AND METHODS

Strains and Growth Conditions

Strains used in this work are derived from the 137c strain of *Chlamydomonas reinhardtii* except *dum22*, which is a hybrid from *C. reinhardtii* × *C. smithii* (Matagne and Remacle, 2002; see Table I for details). Cells were routinely grown at 25°C in Tris-acetate-phosphate medium (Gorman and Levine, 1965) under 70 μmol m^{-2} s^{-1} continuous white light and harvested

at a density of 4×10^6 cells mL^{-1}. Cell density was monitored using a coulter counter (Coulter Electronics, Harpenden Herts, UK).

Pigment Analysis

Pigments were extracted from whole cells in ethanol and debris were removed by centrifugation at 10,000*g* for 15 min. The Chl (*a* and *b*) concentration was determined according to Lichtenthaler (1987) with a lambda 20 UV/Vis spectrophotometer (Perkin Elmer, Norwalk, CT). Twenty-five microliters of pigment extract was subjected to reverse-phase HPLC analysis using a set-up comprising a 616 pump, a 717 plus autosampler, and a 996 online photodiode array detector (Waters, Milford, MA). A Nova Pak C18, 60A column (150-mm length, 4-μm pore size) was used for separation. Acquisition and data treatment were performed using the Millenium software (Waters). Pigments were eluted during 2 min with a gradient from 100% (v/v) solvent A (80% [v/v] methanol and 20% [v/v] 0.5 M ammonium acetate [pH 7]) to 100% (v/v) solvent B (90% [v/v] acetonitrile in water), then during 20 min with a gradient from 100% (v/v) solvent B to 31% (v/v) solvent B and 69% (v/v) solvent C (ethyl acetate) and during 3 min with a gradient from the latter solvent mixture to 100% (v/v) solvent A. The solvent flow rate was 1 mL min^{-1}. Concentrations of individual pigments were determined using authentic references prepared by chromatography on silica gel thin-layer plates (Chl *a* and *b*) or pigments purchased from DHI-Water and Environment (Horstholm, Denmark).

Protein Content

Protein content was determined according to the method of Bradford (1976).

ATP Determination

ATP was extracted according to Gans and Rebeille (1990). ATP cellular level was determined using the Enliten luciferase/luciferin kit (Promega, Madison, WI).

Redox Absorbance Difference Spectra

The isolation of total membrane fractions was conducted according to Remacle et al. (2001), and 60% (v/v) glycerol was added to the preparation. The amounts of Cyt *b-559* (high potential + low potential forms) and Cyt *f* were determined by redox difference spectra as by Mizusawa et al. (1995) using extinction coefficients $\epsilon_{559nn} = 15\ mM^{-1}\ cm^{-1}$ for Cyt *b-559* and $\epsilon_{554nn} = 26\ mM^{-1}\ cm^{-1}$ for Cyt *f* (Metzger et al., 1997). P700 was determined according to Melis and Brown (1980), using $\epsilon_{700nn} = 64\ mM^{-1}\ cm^{-1}$.

State Transition Treatments

Cells were placed in state 1 conditions by incubation for 15 min either under white light (70 μmol $m^{-2}\ s^{-1}$) in the presence of 10 μM DCMU or under far-red light (>705 nm, fluence rate of 60 W m^{-2}). The transition to state 2 was achieved by anaerobic incubation in darkness under nitrogen atmosphere for 20 min (Bulté et al., 1990).

Oxygen Evolution and Fluorescence Emission Measurements

Respiration and photosynthesis were measured as O_2 exchange rates using a Clark-type oxygen electrode at 25°C (Chlorolab 2, Hansatech Instruments, King's Lynn, UK). The actinic light was provided by light-emitting diodes with an emission maximum around 650 nm. Light saturation curves were obtained by measuring O_2 exchange rates during successive 2-min illumination periods with PPFDs increasing stepwise from 0 to 1,000 μmol $m^{-2}\ s^{-1}$. Chl concentration was 2 to 3 μg mL^{-1}.

Changes of fluorescence yield associated with the transition to state 1 were measured in the chamber used for the O_2 recordings using a modulated fluorometer (type MFMS, Hansatech Instruments). The analytical light was provided by light-emitting diodes with an emission maximum of 580 nm and PPFD of 0.5 μmol $m^{-2}\ s^{-1}$. Actinic white light was provided by a tungsten-halogen lamp (Intralux 500-H, Volpi AG, Urdorf-Zürich). The final PPFD was adjusted using neutral filters.

Fast fluorescence rise kinetics associated with PQ photoreduction were recorded at room temperature under continuous excitation using a portable fluorometer (Handy-PEA, Hansatech Instruments) equipped with an accessory for liquid suspension measurements. Actinic light at 650 nm was set at a PPFD of 1,000 μmol $m^{-2}\ s^{-1}$, and Chl concentration of the algal samples was adjusted to a constant value of 20 μg mL^{-1}. Data acquisition rates of 10 μs during the first 2 ms and fast stabilization (50 μs) of the light-emitting photodiodes allowed accurate determination of F_o and, hence, of F_v/F_m ratios (Srivastava et al., 1995). However, F_v/F_m ratios of wild-type cells were lower than previously reported (around 0.6 instead of 0.7–0.75 in Srivastava et al., 1995). This was related to the relatively short adaptation time of the algae in liquid medium (around 4 h) used in this study because we observed a slow increase of F_v/F_m values during growth in liquid medium over days (data not shown). Apparent values of the number of oxidized PQ molecules per PSII were calculated according to Malkin and Kok (1966; see also Bennoun, 2001) as $1/2(A_C - A_{DCMU})/A_{DCMU}$, where A_C and A_{DCMU} are the complementary areas above the fluorescence induction curves of control and DCMU-treated samples, respectively (DCMU was prepared in ethanol and the final concentration was 5 μM in 0.5% [v/v] ethanol).

Fluorescence emission spectra at 77 K were recorded using a LS 50B spectrofluorometer (Perkin Elmer). The excitation wavelength was 440 nm and excitation, and emission slits were 10 and 5 nm, respectively. A broad blue filter (CS-4-96, Corning, Corning, NY) was placed between the excitation window and the sample to minimize stray light. Cells were treated to induce state transitions before freezing in liquid nitrogen. Chl concentration was lower than 2 μg mL^{-1}, and it was verified that no changes in the intensity ratio of the 685- and 715-nm emission bands arose from reabsorption artifacts. Spectra were corrected for the wavelength-dependent photomultiplier response.

Analysis of LHCII Protein Complexes

State 1 or state 2 conditions were applied as described above, and the phosphorylation states of LHCII were stabilized by incubating the cells (5×10^6 cells mL^{-1}) during 5 min in darkness at 4°C in the presence of 600 μM *p*-benzoquinone (adapted from Bulté and Wollman, 1990). Cells were then harvested and suspended in the extraction buffer (25 mM HEPES-KOH [pH 7.0], 5 mM $MgCl_2$, 300 mM Suc, and 1 mM phenylmethylsulfonyl fluoride) and total membranes were prepared as described (Remacle et al., 2001). Ten micrograms of proteins of membrane fractions was separated by SDS-PAGE using 15% (w/v) acrylamide gels containing 6 M urea and electroblotted to polyvinylidene difluoride membrane according to standard protocols. Phosphorylated proteins were detected using rabbit polyclonal antibodies to phospho-Thr (Zymed Laboratories Inc., Am Uden, The Netherlands) and the ECL kit using anti-rabbit horseradish peroxidase-conjugated antibodies (Roche Applied Science, Vilvoorde, Belgium). The molecular size of the proteins was calculated by comparison with known markers (Dual Color protein standards, Bio-Rad Laboratories, Hercules, CA).

Photo-Acoustic Spectroscopy

Photo-acoustic measurements of ES by PSI were performed as described in detail by Ravenel et al. (1994). In brief, cells deposited on a cellulose nitrate/acetate filter were illuminated by a modulated light that exclusively excites PSI ($\lambda > 715$ nm, modulation frequency value selected between 10 and 800 Hz with a constant integrated fluence rate of 21 W m^{-2}). Heat dissipation was measured as the amplitude A of the generated acoustic wave (photothermal signal) in synchronicity with the exciting modulated light. After about 30 s, a saturating continuous white light (1,400 μmol $m^{-2}\ s^{-1}$) was superimposed on the modulated light, which caused an increase of the photothermal signal to an amplitude A^{max} as the absorbed modulated light energy was then dissipated as heat. ES was calculated as $ES = (A^{max} - A)/A^{max}$. It was verified that the intensity of the modulated light was weak enough to allow maximal ES to be measured (i.e. the modulated light could be considered as analytic in our conditions).

ACKNOWLEDGMENT

The authors thank Prof. Francis-André Wollman for helpful suggestions during experiments on state transitions.

Received June 10, 2003; returned for revision June 30, 2003; accepted July 21, 2003.

LITERATURE CITED

Allen JF (1992) Protein phosphorylation in regulation of photosynthesis. Biochim Biophys Acta **1098:** 275–335

Bartoli CG, Pastori GM, Foyer CH (2000) Ascorbate biosynthesis in mitochondria is linked to the electron transport chain between complexes III and IV. Plant Physiol **123:** 335–343

Bennoun P (1982) Evidence for a respiratory chain in the chloroplast. Proc Natl Acad Sci USA **79:** 4352–4356

Bennoun P (2001) Chlororespiration and the process of carotenoid biosynthesis. Biochim Biophys Acta **1506:** 133–142

Bradford MM (1976) A rapid and sensitive method for the quantification of microgram quantities of protein utilizing the principle of protein-dye binding. Anal Biochem **72:** 248–254

Bulté L, Gans P, Rebeillé F, Wollman FA (1990) ATP control on state transitions *in vivo* in *Chlamydomonas reinhardtii*. Biochim Biophys Acta **1020:** 72–80

Bulté L, Wollman FA (1990) Stabilization of states I and II by *p*-benzoquinone treatment of intact cells of *Chlamydomonas reinhardtii*. Biochim Biophys Acta **1016:** 253–258

Canaani O, Schuster G, Ohad I (1989) Photoinhibition in *Chlamydomonas reinhardtii*: effect on state transition, intersystem energy distribution and photosystem I cyclic electron flow. Photosynth Res **20:** 129–146

Cardol P, Matagne RF, Remacle C (2002) Impact of mutations affecting ND mitochondria-encoded subunits on the activity and assembly of complex I in *Chlamydomonas*: implication for the structural organization of the enzyme. J Mol Biol **319:** 1211–1221

Colin M, Dorthu MP, Duby F, Remacle C, Dinant M, Wolwertz MR, Duyckaerts C, Sluse F, Matagne RF (1995) Mutations affecting the mitochondrial genes encoding the cytochrome oxidase subunit I and apocytochrome b of *Chlamydomonas reinhardtii*. Mol Gen Genet **249:** 179–184

Delepelaire P, Wollman FA (1985) Correlations between fluorescence and phosphorylation changes in thylakoid membranes of *Chlamydomonas reinhardtii* in vivo: a kinetic analysis. Biochim Biophys Acta **809:** 277–283

Delosme R, Olive J, Wollman FA (1996) Changes in light energy distribution upon state transitions: an in vivo photoacoustic study of the wild type and photosynthesis mutants from *Chlamydomonas reinhardtii*. Biochim Biophys Acta **1273:** 150–158

Finazzi G, Furia A, Barbagallo RP, Forti G (1999) State transitions, cyclic and linear electron transport and photophosphorylation in *Chlamydomonas reinhardtii*. Biochim Biophys Acta **1413:** 117–129

Finazzi G, Rappaport F, Furia A, Fleischmann M, Rochaix JD, Zito F, Forti G (2002) Involvement of state transitions in the switch between linear and cyclic electron flow in *Chlamydomonas reinhardtii*. EMBO Rep **3:** 280–285

Fleischman MM, Ravanel S, Delosme R, Olive J, Zito F, Wollman FA, Rochaix JD (1999) Isolation and characterization of photoautotrophic mutants of *Chlamydomonas reinhardtii* deficient in state transition. J Biol Chem **274:** 30987–30994

Gans P, Rebeille F (1990) Control in the dark of the plastoquinone redox state by mitochondrial activity in *Chlamydomonas reinhardtii*. Biochim Biophys Acta **1015:** 150–155

Gorman DS, Levine RP (1965) Cytochrome *f* and plastocyanin: their sequence in the photosynthetic electron transport chain of *Chlamydomonas reinhardtii*. Proc Natl Acad Sci USA **94:** 3436–3441

Hoefnagel MHN, Atkin OK, Wiskich JT (1998) Interdependence between chloroplasts and mitochondria in the light and the dark. Biochim Biophys Acta **1366:** 235–255

Joët T, Cournac L, Peltier G, Havaux M (2002) Cyclic electron flow around photosystem I in C3 plants: in vivo control by the redox state of chloroplasts and involvement of the NADH-dehydrogenase complex. Plant Physiol **128:** 760–769

Joliot P, Joliot A (2002) Cyclic electron transfer in plant leaf. Proc Natl Acad Sci USA **99:** 10209–10214

Lichtenthaler HK (1987) Chlorophylls and carotenoids: pigments of photosynthetic biomembranes. Methods Enzymol **148:** 350–382

Malkin S, Canaani O (1994) The use and characteristics of the photoacoustic method in the study of photosynthesis. Annu Rev Plant Physiol Plant Mol Biol **45:** 493–526

Malkin S, Kok B (1966) Fluorescence induction studies in isolated chloroplasts: I. Number of components involved in the reaction and quantum yields. Biochim Biophys Acta **126:** 413–432

Matagne RF, Michel-Wolwertz MR, Munaut C, Duyckaerts C, Sluse F (1989) Induction and characterization of mitochondrial DNA mutants in *Chlamydomonas reinhardtii*. J Cell Biol **108:** 1221–1226

Matagne RF, Remacle C (2002) The genetics and molecular biology of mitochondria in *Chlamydomonas*. Recent Res Dev Plant Biol **2:** 15–32

Melis A, Brown JS (1980) Stoichiometry of system I and system II reaction centers and of plastoquinones in different photosynthetic membranes. Proc Natl Acad USA **77:** 4712–4716

Metzger SU, Cramer WA, Whitmarsh J (1997) Critical analysis of the extinction coefficient of chloroplast cytochrome *f*. Biochim Biophys Acta **1319:** 233–241

Mizusawa N, Ebina M, Yamashita T (1995) Restoration of the high potential form of cytochrome b-559 through the photoreactivation of Tris-inactivated oxygen-evolving center. Photosynth Res **45:** 71–77

Peltier G, Cournac L (2002) Chlororespiration. Annu Rev Plant Physiol Plant Mol Biol **53:** 523–550

Ravenel J, Peltier G, Havaux M (1994) The cyclic electron pathways around photosystem I in *Chlamydomonas reinhardtii* as determined in vivo by photoacoustic measurements of energy storage. Planta **193:** 251–259

Rebeille F, Gans P (1988) Interaction between chloroplasts and mitochondria in microalgae. Plant Physiol **88:** 973–975

Remacle C, Duby F, Cardol P, Matagne RF (2001) Mutations inactivating mitochondrial genes in *Chlamydomonas reinhardtii*. Biochem Soc Trans **29:** 442–445

Remacle C, Matagne R (2002) The genetics and molecular biology of mitochondria in *Chlamydomonas*. *In* SG Pamalai, ed, Recent Research Development in Plant Biology. Research Signpost, Kerala, India, pp 15–32

Smirnoff N (2000) Ascorbate biosynthesis and function in photoprotection. Philos Trans R Soc Lond B **355:** 1455–1464

Srivastava A, Strasser RJ, Govindjee (1995) Polyphasic rise of chlorophyll *a* fluorescence in herbicide-resistant D1 mutants of *Chlamydomonas reinhardtii*. Photosynth Res **43:** 131–141

Vallon O, Bulté L, Dainese P, Olive J, Bassi R, Wollman FA (1991) Lateral redistribution of cytochrome b6/f complexes along the thylakoid membranes upon state transitions. Proc Natl Acad Sci USA **88:** 8262–8266

Vallon O, Wollman FA, Olive J (1986) Lateral distribution of the main protein complexes of the photosynthetic apparatus in *Chlamydomonas reinhardtii* and in spinach: an immunocytochemical study using intact thylakoid membranes and a PSII enriched membrane preparation. Photobiochem Photobiophys **12:** 203–220

Wheeler GL, Jones MA, Smirnoff N (1998) The biosynthetic pathway of vitamin C in higher plants. Nature **393:** 365–369

Wollman FA (2001) State transitions reveal the dynamics and flexibility of the photosynthetic apparatus. EMBO J **20:** 3623–3630

Wollman FA, Delepelaire P (1984) Correlation between changes in light energy distribution and changes in thylakoid membrane polypeptide phosphorylation in *C. reinhardtii*. J Cell Biol **98:** 1–7